Reviewed

Simulation study of the impact of QZSS on land survey

Munekane Hiroshi, Yuki Kuroishi, Yuki Hatanaka, *Geographical Survey Institute*
Hisashi Miyazaki, *Japan Association of Surveyors*
munekane@gsi.go.jp

BIOGRAPHY

Hiroshi Munekane is a Senior Researcher at the Geographical Survey Institute, Japan (GSI). He received his D. Sci. from University of Tokyo, Japan in geophysics in 2001. He joined GSI in 2001, and has been working on error analysis of GPS-derived position time series.

Yuki Kuroishi is Head of Space Geodesy Research Division at GSI. In 1994, he received his D. Sci. from Kyoto University in geophysics. He joined GSI in 1986 and has been working on research in physical geodesy, especially on vertical datum, and gravity field and geoid modeling.

Yuki Hatanaka is a Senior Researcher at GSI. He received his D. Sci. from Hokkaido University, Japan in geophysics in 2002. He joined GSI in 1991, and has been working on research and development on GPS data analysis for geodesy.

Hisashi Miyazaki received his B. Eng. from University of Chiba, Japan in applied chemistry in 1994. He has been working at Japan Association of Surveyors (JAS) since 2002. At JAS he works as a survey consultant. He is also in charge of calibration of survey instruments.

ABSTRACT

The Quasi-Zenith Satellite System (QZSS) is a dedicated Japanese geodetic satellite system under development. We quantitatively evaluate through numerical simulation how QZSS can enhance GPS applicability in land survey in those areas where sky visibilities are limited. For the numerical simulation, we have developed software, called SPSS, for simulating observational data of general global navigation satellite systems including QZSS in any designed orbits. SPSS is composed of three modules, namely, 1) the orbit generation module where tabular positions for arbitrary satellites are generated based on their assigned orbit elements, 2) the observable generation module where observation data for selected satellite systems at an observation site are generated, 3) the visualization module where supplemental information for evaluating positioning accuracies, such as PDOP and number of visible satellites, are plotted. The outputs of SPSS are satellite positions and observation data in commonly-used formats. Users may analyze those data with generic positioning software so that they may evaluate positioning accuracies. To evaluate the enhancement of GPS applicability in land survey with QZSS, we conducted a numerical simulation using SPSS for two different cases under severe meteorological disturbances. In one case, we simulated observations at urban and mountain areas where sky visibilities are poor, and evaluated the impact of QZSS enhancement of GPS land survey on positioning accuracy. In the other case, we systematically changed the elevation cut-off angle in the GPS analysis to evaluate the impact of QZSS enhancement of GPS land survey on requirement for minimum satellite elevation angle for maintaining certain positioning accuracies. We obtained following results: 1) QZSS observations considerably improve positioning accuracies at those sites where satellite visibilities are poor, 2) ignoring the tropospheric delay effects may result in large biases (up to 5cm) in the estimated positions, especially in the vertical component, even for a short baseline which are not mitigated even with QZSS observations, and 3) higher minimum elevation angles of visible satellites will be tolerated for given precision requirement on land survey when QZSS observations are available.

INTRODUCTION

The Quasi-Zenith Satellite System (hereafter referred to as QZSS) is a dedicated Japanese geodetic satellite system under development. In full constellation, it consists of three satellites orbiting at the altitude similar to geostationary satellites but in inclined planes so that at least one satellite will stay close to the zenithal direction over Japan. Thus, this satellite system is expected to

enhance GPS availability in urban areas and mountainous regions where it is difficult to utilize satellite systems due to limited sky visibilities.

One of possible applications of QZSS will be land survey where QZSS is supposed to complement the Global Positioning System (GPS). The QZSS satellites are designed to transmit GPS-compatible signals so that surveyors may use them as additional GPS satellites. QZSS, with its enhanced visibility, will contribute to enhancement of GPS applicability in land survey in those areas where it is difficult to observe a sufficient number of GPS satellites due to poor sky visibilities.

In this study, we quantitatively evaluate through numerical simulation how QZSS can enhance GPS applicability in land survey in those areas where sky visibilities are limited.

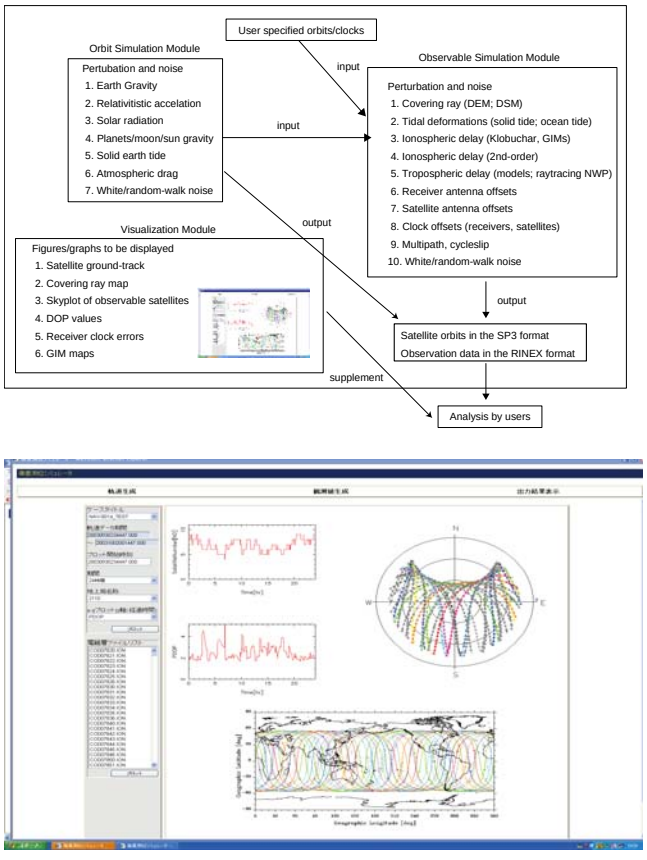

Figure 1 (Top) Schematics of functions of SPSS. (Bottom) A screenshot from the software. Supplemental figures such as a sky plot, time series of PDOP and number of visible satellites, and ground-track map of the satellites are displayed.

SATELLITE POSITIONING SYSTEM SIMULATOR (SPSS)

For the numerical simulation, we have developed software for simulating observational data of general global navigation satellite systems including QZSS in any designed orbits. The software, named ``Satellite Positioning System Simulator (SPSS)'', is composed of three modules, namely, 1) the orbit generation module where tabular positions for satellites are generated based on their arbitrarily assigned orbit elements, 2) the observable generation module where observation data for selected satellite systems at any observation site are generated, 3) the visualization module where supplemental information for evaluating positioning accuracies, such as PDOP and number of visible satellites, are plotted. The outputs of SPSS are satellite positions in the SP3 format (Remondi, 1991) and observation data in the RINEX format (Gurtner, 1994). Users may analyze those data with generic positioning software so that they may evaluate positioning accuracies. In the simulation using SPSS, one may add various kinds of errors on both satellite positions and observation data so that one may reproduce realistic positioning errors. In Figure 1 we briefly summarize the functions of SPSS along with various optional input and output.

NUMERICAL SIMULATION-OUTLINE

To evaluate the QZSS enhancement of GPS applicability in land survey, we conducted a numerical simulation using SPSS for two different cases in Kanto and Tokai region. In one case, we simulated observations at urban and mountain areas where sky visibilities are poor, and evaluated the impact of QZSS enhancement of GPS land survey on positioning accuracy. In the other case, we systematically changed the elevation cut-off angle in the GPS analysis to evaluate the impact of QZSS enhancement of GPS land survey on requirement for minimum satellite elevation angle for maintaining certain positioning accuracies.

In Table 1, we summarize the orbital elements of the QZSS satellites used in this simulation. We assumed that the QZSS satellites are in full constellation with three satellites on orbit. Figure 2 shows examples of the sky-plot and number of available satellites at a station in Japan. In this configuration, one satellite will always stay around the zenithal direction, and one or two satellites will remain visible where sky visibilities are high.

Table 1 Orbital elements of the QZSS satellites used in this simulation

Number of satellites	3
Semi-major axis	42164km
Eccentricity	0.0998
Argument of perigee	270 degree
Right ascension of ascending node	0, 120, 240 degree

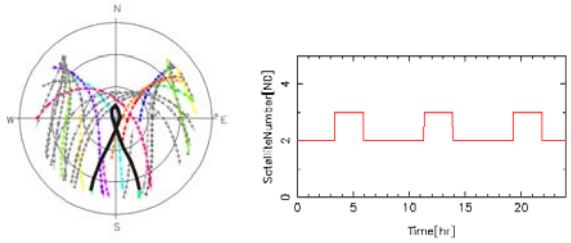

Figure 2 Example of QZSS observations over Japan. (Left) Skyplot at the station. Black line denotes the duplicated trajectory of the QZSS satellites. (Right) Number of visible QZSS satellites. This example is calculated at Tsukuba where sky visibility is high.

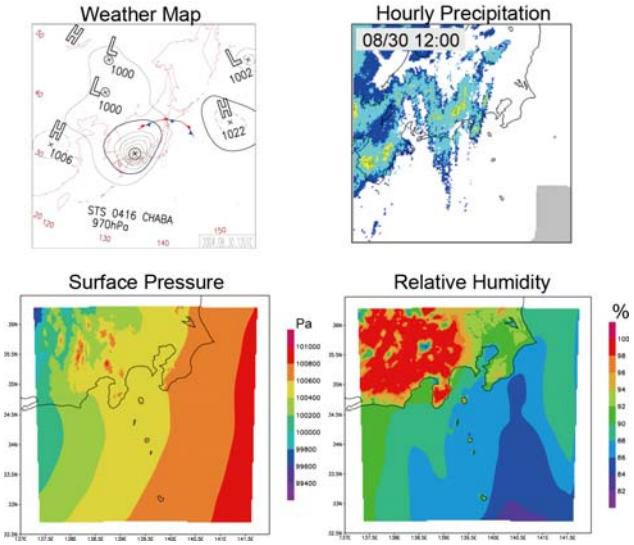

Figure 3 Weather condition maps on the simulated day. (Top left) Weather system at noon. The typhoon in the western Japan created eastward pressure gradient in Kanto region. (Top right) Hourly precipitation at noon revealed by ground observations and echo measurements. (Bottom left) Surface pressure at noon in the numerical weather model. Eastward pressure gradients observed in the weather map are well-reproduced. (Bottom right) Relative humidity at noon. The wide high precipitation area west to Tokyo can be identified as the area with high humidity.

We simulated the observation data on Aug. 30, 2004 when we had severe meteorological disturbances due both to the typhoon and weather front. In the simulation, we employed a fine-resolution (2 km x2 km spatial and 1h temporal) numerical weather model to reproduce reasonable tropospheric delays at simulated sites.

Figure 3 shows the weather conditions at noon of the day with maps of weather system, hourly precipitation, and maps of surface pressure and relative humidity in the numerical weather model. The typhoon centered in the western Japan created eastward pressure gradient in Kanto and Tokai region and wide high precipitation area west to Tokyo. In the numerical simulation model, one can see that those characteristics are well reproduced.

In Table 2 we summarized other conditions used in the numerical simulation.

Table 2 Summary of conditions used in numerical simulation in this study.

Date	August 30, 2004	
Orbit generation		
GPS satellite positions	IGS final orbits	
QZSS satellite positions	Summarized in Table 1	
Earth gravity model	EGM96 (Lemoine et al., 1998)	
Relativistic acceleration	Considered	
Solar wind pressure model	GPS	T20/30
	QZSS	Cannon ball
Solid earth tide model	IERS96	
Additional noise on satellite positions	GPS	Broadcast orbits are used in the analysis.
	QZSS	White noise with SD of 2m in each direction
Observable generation		
Solid earth tide model	IERS96 (McCarthy, 1996)	
Ionospheric delay model	CODE GIM (Schaer et al., 1995)	
Tropospheric delay	Ray-traced tropospheric delay calculated with fine-scale numerical weather models	
Noise	Independent noise	White noise with SD of 2.4 mm on both L1 and L2.
	Coherent (ionosphere) noise	White noise with SD of 0.4 mm/(baseline length in km) on L1, and corresponding noise on L2.

NUMERICAL SIMULATION-CASE A: IMPACT OF QZSS ENHANCEMENT OF GPS LAND SURVEY ON POSITIONING ACCURACIES

Here we investigate the impact of QZSS enhancement of GPS land survey on positioning accuracy. The impact will be best seen where the sky visibilities are low. Therefore, we studied two areas, one in urban region and the other in mountainous region, where one expect low sky visibilities.

In each area, we selected five different networks, composed of five stations each, corresponding to typical baseline lengths of 2 km, 5 km, 10 km and 15 km. At each station, we used realistic shadow maps so that one may reproduce observations under low sky visibilities. Figures 4 and 5 show the location of networks at respective areas as well as shadow maps applied at corresponding stations. Shadow maps are calculated based on a Digital Surface Model for the urban stations and Digital Elevation Model for the mountainous stations. For the urban stations, the actual shadow maps at stations in the 2 km network are used for the other networks as well.

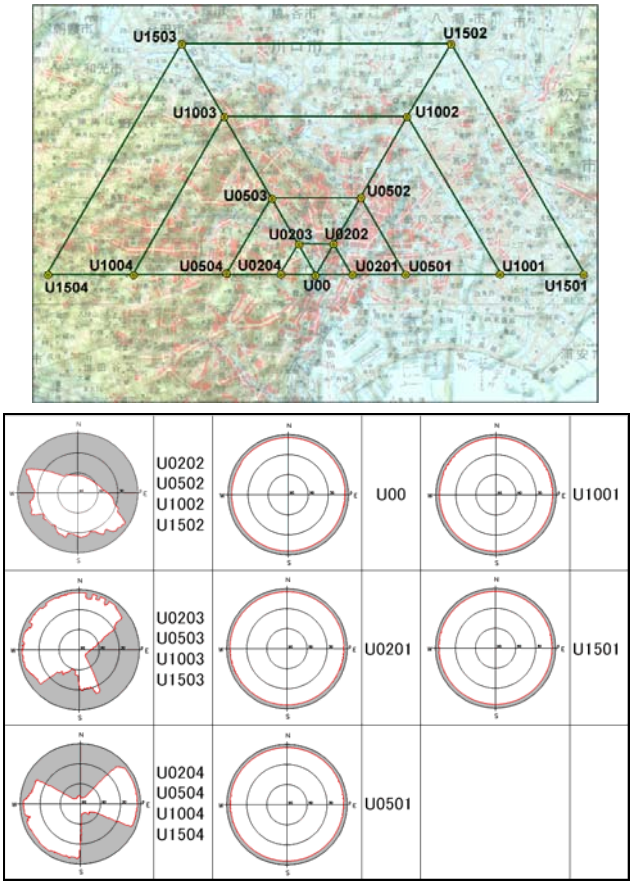

Figure 4 (Top) Location of the simulated areas representing urban environment. (Bottom) Shadow maps applied in the simulation.

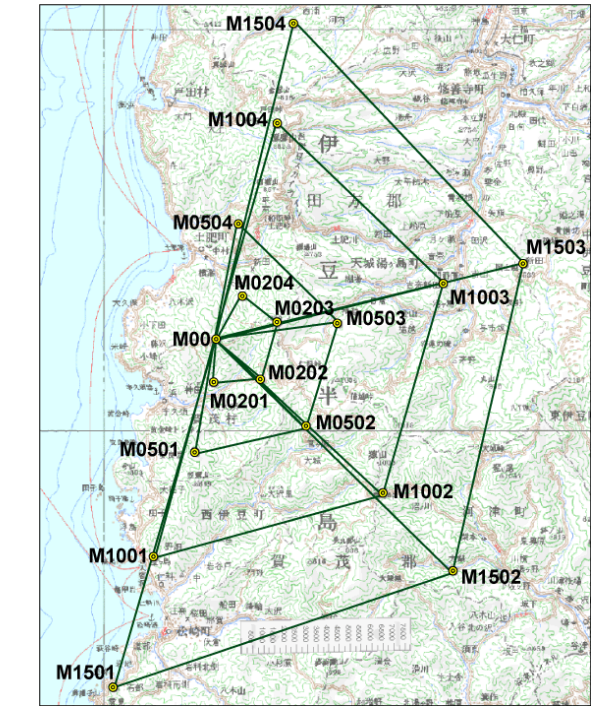

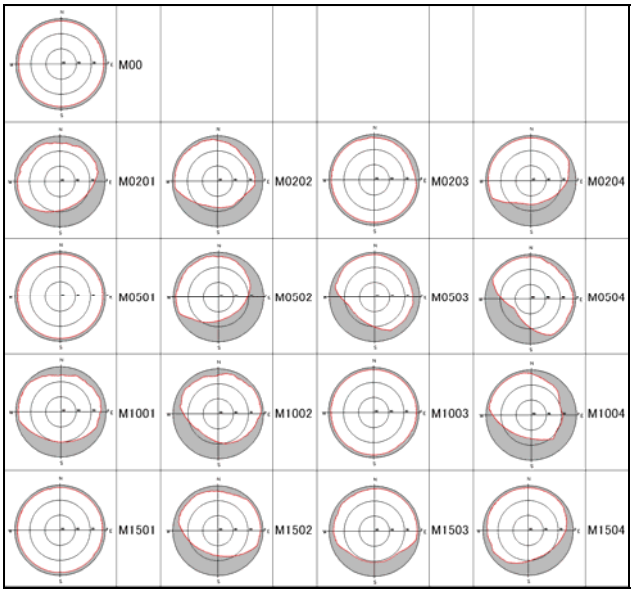

Figure 5 Location of the simulated areas representing mountainous environment and the shadow maps applied in the simulation.

We analyzed the data in the following procedure which is typical of GPS land surveys in Japan: 1) no troposphere delay estimation, 2) L1 analysis with one-hour time window for baselines less than 10 km, and 3) L3 analysis with two-hour time window for baselines longer than 10 km. We set the elevation cut-off angle as 15 deg in the analysis which is a commonly-used for land survey. We used the GAMIT version 10.32 (King and Bock, 2006) for the analysis.

First, we evaluate the impact of QZSS enhancement of GPS land survey on positioning accuracies in terms of the RMS reduction. Figures 6 and 7 show the RMS of positioning errors, i.e., the difference between estimated positions and given positions. Table 3 summarized the reduction in the RMS with complementary QZSS. One can see that the complementary observation of the QZSS satellites significantly improve the positioning accuracies except for the vertical direction in the mountainous area. In the urban area, the reduction in the RMS of the positioning error amounts to 80 % in each horizontal and vertical component. In the mountainous area, one observes reduction of the RMS as high as 65% in the horizontal component. However, in the vertical component, only 26% of reduction is observed which is not significant compared to those observed in the other case.

One may note that the positioning accuracies for the 5 km baselines in the urban area are notably worse than those for other baselines. This is attributed to a couple of unstable baseline solutions caused by excessive data editing triggered by severe coherent (ionosphere) noises for those baselines. Note that even in these extreme cases, additional QZSS observations successfully stabilize baseline solutions.

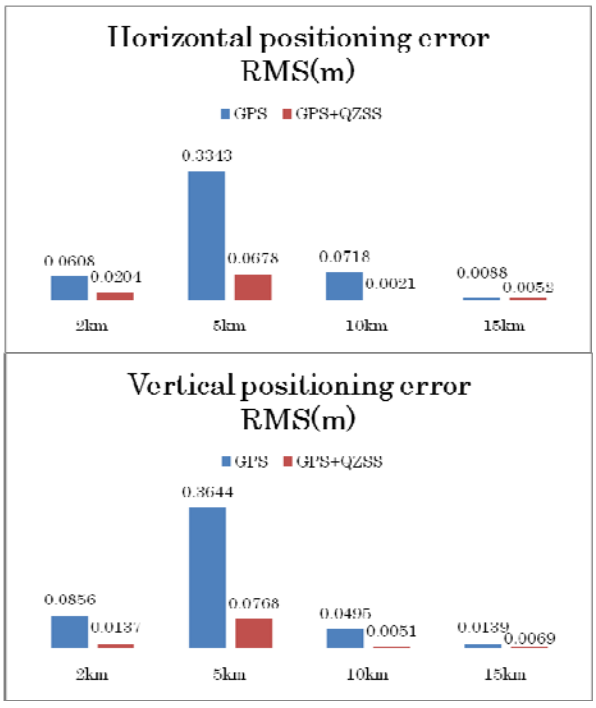

Figure 6 Positioning errors in the urban area. Blue boxes show the RMS with standalone GPS and red boxes show those with complementary QZSS. Note that complementary QZSS significantly reduce the positioning errors.

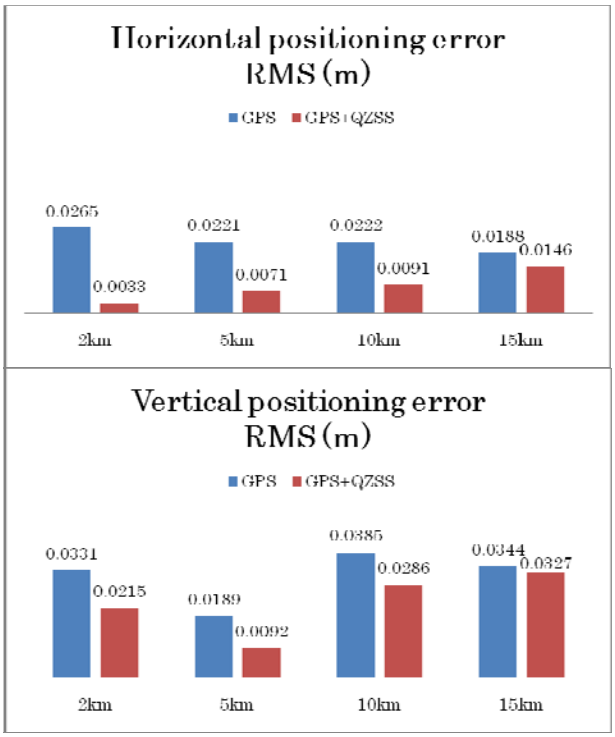

Figure 7 Positioning errors in the mountainous area. Legends are the same as in Figure 5.

Table 3 Summary of the RMS of positioning errors and reduction of the RMS due to the complementary QZSS observations.

Urban	GPS only (m)	GPS+QZSS (m)	Reduction (%)
Horizontal	0.119	0.0239	79.8
Vertical	0.128	0.0256	80.0

Mountainous	GPS only (m)	GPS+QZSS (m)	Reduction (%)
Horizontal	0.0224	0.00853	64.5
Vertical	0.0312	0.0230	26.3

Next, we evaluate the impact of QZSS enhancement of GPS land survey on positioning accuracies in terms of ``invalid session rate''. In land survey, validity of estimated positions will be checked by some indices such as baseline repeatability or loop closure. Those sessions that do not meet the criteria will be considered as invalid observations, and observation should be carried out again. Here, we tentatively set those sessions whose positioning errors exceed 2 cm in horizontal component or 3cm in the vertical component as invalid, and see whether complementary QZSS will reduce invalid session rate. In Table 4, we summarized the invalid session rate for the urban and mountainous areas. In the urban area, the

invalid session rate was reduced from 40.4 % to 3.3 %. However, in the mountainous area, it does not improve as significant as in the urban case, reflecting limited improvement in the vertical positioning accuracies in this area.

Table 4 Invalid session rate observed in the simulation for the urban and mountainous area.

	GPS only(%)	GPS+QZSS(%)
Urban	40.4	3.3
Mountainous	57.6	45.0

To investigate causes behind the low RMS reduction for the vertical component in the mountainous area, we plotted the histograms of the positioning errors for 5 km baselines in the mountainous area in Figure 8. One can see that the positioning errors in the vertical component are biased, and the complementary QZSS observations do not mitigate the biases.

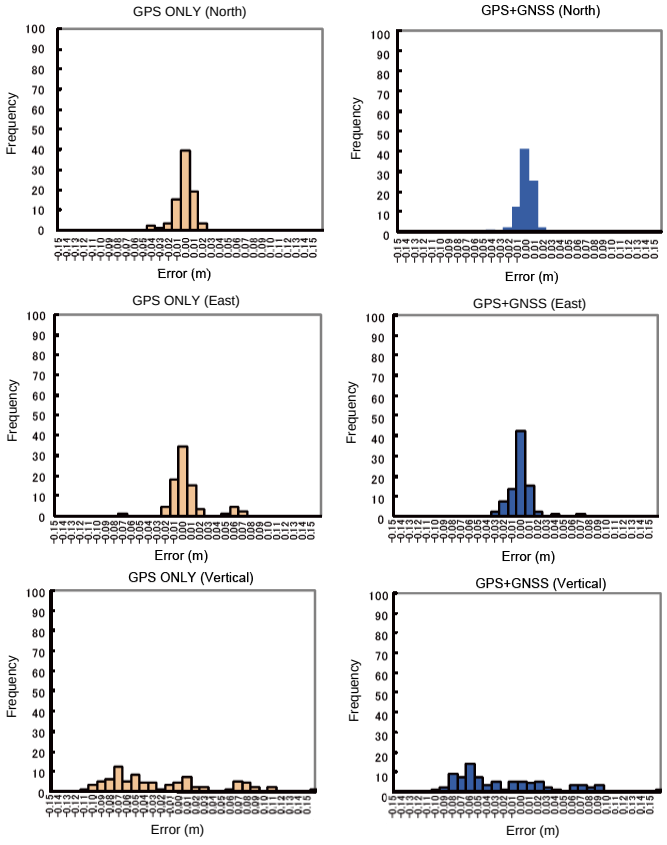

Figure 8 Histograms of the positioning errors. Note that the errors are biased in the vertical component.

It is likely that the differential tropospheric delays at both ends of the baselines that are induced under severe meteorological disturbances are responsible for the observed biases since the biases are not observed on a quiet day. In the following, we test this hypothesis by directly evaluating the differential tropospheric delays from numerical weather models to see whether they are sufficiently large to account for the observed large height biases.

For this purpose, we investigated the differential tropospheric delays for 5 km baselines as a typical example. We first calculated the total tropospheric delays at end stations using numerical meteorological models. Then we subtracted a priori tropospheric delays given by Saastamoinen (1973), which are used in the analysis software, from the total tropospheric delays to obtain the residual tropospheric delays. Finally, we obtained the differential tropospheric delays for each baseline by taking differences of the residual tropospheric delays at both ends. Figure 9 shows the differential tropospheric delays for 5 km baselines. One can see the differential tropospheric delays over 0.015 m are observed for some baselines. According to Beutler et al (1988), a rules-of-thumb relationship between the differential tropospheric delay and height error with the ideal sky visibility may be given as:

$$\Delta h = \frac{1}{\sin(\theta_c)} \Delta Z \,, \qquad (1)$$

where Δh , θ_c and ΔZ denote height error, elevation cut-off angle and differential tropospheric delay, respectively. According to equation (1), a differential tropospheric delay of 0.015 m amounts to height error as large as 0.058 m for 15 deg elevation cut-off even with the perfect sky visibility. This result demonstrates that the tropospheric delays for baselines as short as 5 km may not be effectively canceled out and could cause significant height errors under severe meteorological disturbances.

We have confirmed that these biases vanish when one estimates the zenithal tropospheric delay in the GPS analysis, which also indicates that these biases are caused by differential tropospheric delays under the meteorological disturbances.

In this simulation, the large height biases are only observed in the mountainous area where height differences at both ends of baselines are large. Therefore, one may argue that these height biases are limitedly observed in baselines that have large height differences. We checked this possibility by investigating the influence of the height differences at both ends of baselines on the differential tropospheric delays. In Figure 10, we plotted the height differences against differential tropospheric delays. One can see that there's a tendency that the magnitudes of differential tropospheric delays increase with the height differences. However, even for those baselines whose height differences at both ends are only below 50 m, the differential tropospheric delays as large

as 0.01 m are observed. According to equation (1), a differential tropospheric delay of 0.01 m would cause height bias as large as 0.04 m even with the ideal sky visibility, which should not be neglected in land survey.

It is often assumed that for short baselines less than 10 km, the tropospheric delays will be canceled at both ends and do not affect the estimated baseline components. However, this result shows that under severe meteorological disturbances, it is likely that the tropospheric delays for short baselines as small as 5 km, even if height differences at both ends are small, may not be effectively canceled out. Moreover, the complementary QZSS will not mitigate these biases coming from differential tropospheric delays.

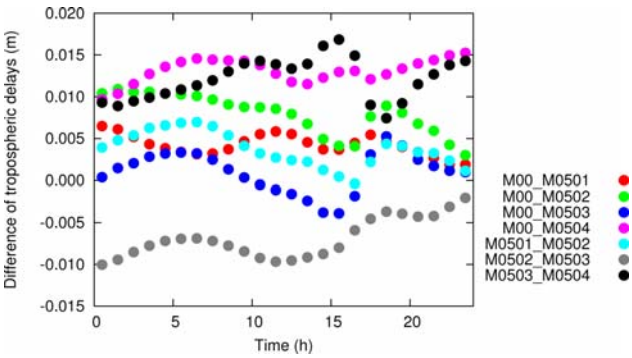

Figure 9 Differential tropospheric delays for 5 km baselines.

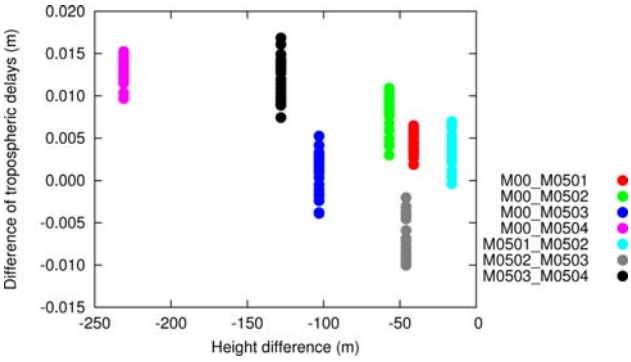

Figure 10 Relationship between the differential tropospheric delays and the height differences.

NUMERICAL SIMULATION-CASE B: IMPACT OF QZSS ENHANCEMENT OF GPS LAND SURVEY ON REQUIREMENT OF MINIMUM ELEVATION ANGLE

We then examine the impact of QZSS enhancement of GPS land survey on requirement of minimum elevation angle of visible satellites. In land survey with GPS, observations of satellites at low elevation angles are critical for achieving high positioning accuracies because those observations ensure a good geometry of visible satellites that will stabilize positioning estimations. Hence, surveyors are advised not to make GPS surveys where maintaining certain minimum elevation angle, 15 degree for example, is difficult. Here we investigate whether the complementary QZSS will mitigate this requirement or not.

For this purpose, we selected four baselines corresponding to typical baseline lengths of 2 km, 5 km, 10 km and 15 km in the urban area near Tokyo (Figure 11). We did not consider shadow maps at each station. Instead, we systematically changed the elevation cut-off angles from 30 degree to 50 degree in the GPS analysis to effectively modify minimum elevation angle, and examined the dependency of positioning accuracies on the minimum elevation angle.

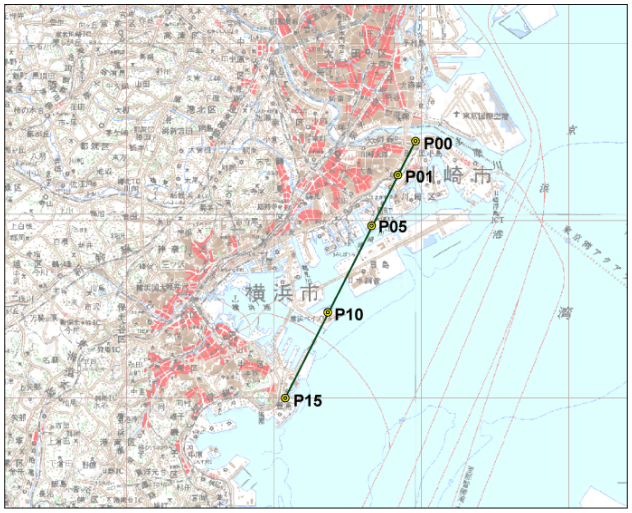

Figure 11 Location of the sites used to investigate the effect of minimum elevation angle of visible satellites on positioning accuracies.

Figure 12 shows the dependency of the positioning error RMS on the minimum elevation angle for two cases: 1) with standalone GPS, and 2) with complementary QZSS. One can see that without QZSS, the positioning error RMS shows sharp increase as the minimum elevation

angle increases. On the other hand, with QZSS the increase of positioning error RMS is suppressed up to minimum elevation angle of 45 degree. In Table 5 we summarized the relation between the invalid session rate and minimum elevation angle. For case 1), one can see that the invalid session rate gradually increases with the increase of minimum elevation angle. On the contrary, for the case 2), the invalid session rate is almost zero for elevation angle below 45 degrees. From these results, we may conclude that higher minimum elevation angle of visible satellites will be tolerated with complementary QZSS for given precision requirement on land survey.

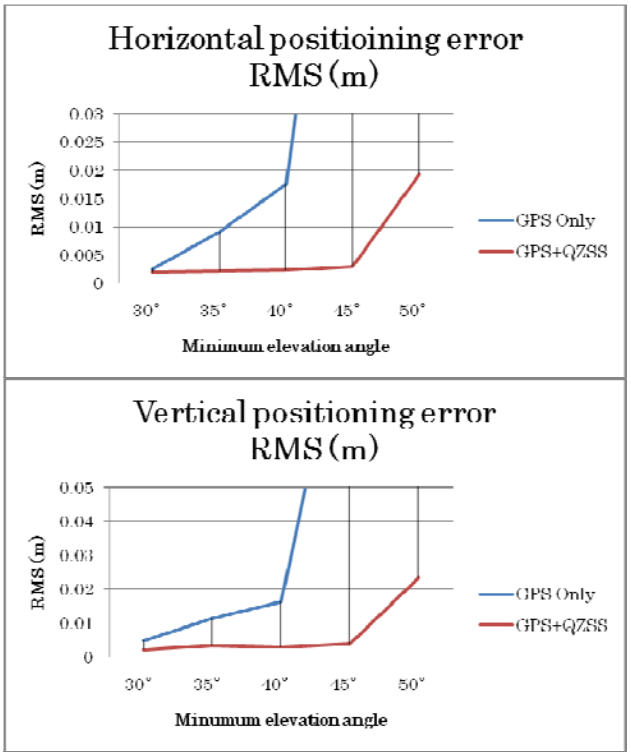

Figure 12 Dependency of positioning error RMS on minimum elevation angle. Blue line denotes the positioning error RMS with standalone GPS, and red line denotes those with complementary QZSS.

Table 5 Relation between the invalid session rate and minimum elevation angle

Minimum Elevation angle	GPS only(%)	GPS+QZSS(%)
30°	0.0	0.0
35°	5.6	0.0
40°	13.1	0.0
45°	28.7	0.0
50°	47.2	4.4

CONCLUSIONS

We obtained following results: 1) complementary QZSS considerably improve positioning accuracies at those sites with poor satellite visibilities; 2) ignoring the tropospheric delay effects may result in large biases (up to 5cm) in the estimated positions, especially in the vertical component, even for a short baseline which are not mitigated by complementary QZSS, and 3) higher minimum elevation angle of visible satellites will be tolerated with complementary QZSS for given precision requirement on land survey.

ACKNOWLEDGMENTS

We would like to thank F. Hayashi for her assistance in figure preparation. This study was funded by ``General Technology Development Project'' of Ministry of Land, Infrastructure, Transport and Tourism.

REFERENCES

Beutler, G., I. Bauersima, W. Gurtner, M. Rothacher, T. Schildknecht, A. Geiger, (1988), Atmospheric refraction and other important biases in GPS carrier phase observations, In "Atmospheric Effects on Geodetic Space Measurements", Monography 12, School of Surveying, University of New South Wales, 15-43.

Gurtner, W. (1994), RINEX: The receiver independent exchange format, GPS world, 5, 48-52.

King, R.W. and Y. Bock (2006), Documentation for the GAMIT GPS Analysis Software, Version 10.32, Massachusetts Institute of Technology, Cambridge, Massachusetts.

Lemoine, F.G., S.C. Kenyon, J.K. Factor, R.G. Trimmer, N.K. Pavlis, D.S. Chinn, C.M. Cox, S.M. Klosko, S.B. Luthcke, M.H. Torrence, Y.M. Wang, R.G. Williamson, E.C. Pavlis, R.H. Rapp, and T.R. Olson (1998), The development of the joint NASA GSFC and NIMA geopotential model EGM96, NASA/TP-1998-206861, NASA Goddard Space Flight Center, Greenbelt, Maryland.

McCarthy, D.D (ed.) (1996), IERS technical note 21, IERS conventions (1996), Observatoire de Paris, Paris.

Remondi, B.W. (1991), NGS second generation ASCII and binary orbit formats and associated interpolated studies, paper presented at the twentieth general assembly, International Union of Geodesy and Geophysics, Vienna.

Saastamoinen, J. (1973), Contribution to the theory of atmospheric refraction, B. Geod., 107, 13-34.

Schaer, S., L. Beutler, L. Mervart, M. Rothacher, and U. Wild (1995), Global and regional ionosphere models using the GPS double difference phase observable, Proceedings of the IGS workshop on special topics on new directions, 77-92, Potsdam.